

WcDT: World-centric Diffusion Transformer for Traffic Scene Generation

Chen Yang¹, Aaron Xuxiang Tian², Dong Chen³, Tianyu Shi^{4*}, Arsalan Heydarian⁵

Abstract—In this paper, we introduce a novel approach for autonomous driving trajectory generation by harnessing the complementary strengths of diffusion probabilistic models (a.k.a., diffusion models) and transformers. Our proposed framework, termed the “World-Centric Diffusion Transformer” (WcDT), optimizes the entire trajectory generation process, from feature extraction to model inference. To enhance the scene diversity and stochasticity, the historical trajectory data is first preprocessed and encoded into latent space using Denoising Diffusion Probabilistic Models (DDPM) enhanced with Diffusion with Transformer (DiT) blocks. Then, the latent features, historical trajectories, HD map features, and historical traffic signal information are fused with various transformer-based encoders. The encoded traffic scenes are then decoded by a trajectory decoder to generate multimodal future trajectories. Comprehensive experimental results show that the proposed approach exhibits superior performance in generating both realistic and diverse trajectories, showing its potential for integration into automatic driving simulation systems.

Index Terms—Traffic scene generation, diffusion probabilistic models, transformer, autonomous driving.

I. INTRODUCTION

Autonomous driving represents a cutting-edge technology set to revolutionize transportation, freeing drivers from exhausting driving and mitigating traffic congestion by enabling vehicles to operate with little or no human intervention [1]–[4]. The development of autonomous driving algorithms often involves a process of trial and error, as researchers seek to optimize performance and enhance safety [5]–[7]. However, the validation of autonomous vehicles (AVs) through real-world testing presents significant challenges. Beyond the substantial time investment required due to the rarity of critical incidents, real-world testing also involves complex safety, regulatory, and cost considerations [8], [9].

As the development of autonomous driving systems (ADS) progresses, simulators play a pivotal role in the design and evaluation process [10]. These simulators offer cost-effective

tools and various traffic scenarios to test driving algorithms, providing controllable environments for experimentation and refinement [11], [12]. To ensure the effective development of AVs, these simulators should be highly realistic, accurately replicating real-world traffic scenarios and driver behaviors to enable effective translation to real-world applications [13]. However, a challenge arises as current driving simulators commonly generate agent behaviors through two primary methods: replaying recorded driving logs or employing heuristic-based controllers [13], [14]. These approaches may restrict the diversity and unpredictability of driving behaviors observed in real-world scenarios, thereby affecting the comprehensiveness of the testing and validation processes for ADS [15].

Recently, multimodal motion prediction approaches [16]–[22] have demonstrated remarkable efficacy in traffic scene generation. These methods, often leveraging efficient fusion strategies or employing encoder-decoder networks with Transformer architectures, have yielded promising results, particularly notable in competitions such as the Waymo Open Dataset Motion Prediction Challenge [23]. However, these methods face limitations in generating actions for all agents based on comprehensive global information and cannot spontaneously generate varied actions [16].

On the other hand, there has been a notable trend toward leveraging generative adversarial networks (GANs) [24]–[26] and Variational Auto-Encoders (VAEs) [27], [28] to create traffic scenes for ADS. However, these methods encounter several limitations. First, the behaviors generated by these models seem plausible as they primarily mirror the distribution of the training data and lack diversity [13]. Additionally, the training process for GANs can be unstable due to adversarial learning [15]. Moreover, most current generative approaches do not effectively utilize the local smoothness of agent trajectories, leading to unrealistic outcomes [15]. Finally, these methods tend to concentrate on predicting future paths for individual vehicles [24]–[26], neglecting the comprehensive representation of all agent types within a scene. More recently, diffusion probabilistic models also referred to as diffusion models, have emerged as a promising framework for generating realistic and diverse traffic scenarios [13], [15], [29], [30]. These approaches conceptualize traffic scene generation as an inverse diffusion process by removing noise from a random distribution. However, it is important to note that these approaches typically require input features to be transformed into Frenet coordinates centered on each agent during the data preprocessing stage to accurately capture the motion dynamics of various agents within the scene [16]. In addition, a notable limitation of these approaches is their tendency to output only

¹Chen Yang is with the Department of Computer Science and Informatics, Cardiff University, Cardiff, UK. Email: yc19970530@gmail.com.

²Aaron Xuxiang Tian is with the Information Networking Institute, Carnegie Mellon University, Pittsburgh, PA, 15213, USA. Email: aarontian00@gmail.com.

³Dong Chen is with Environmental Institute & Link Lab & Computer Science, University of Virginia, Charlottesville, VA, 22903, USA. Email: dqc4vv@virginia.edu.

⁴Tianyu Shi is with Transportation Research Institute, University of Toronto. Email: ty.shi@mail.utoronto.ca.

⁵Arsalan Heydarian is with Link Lab & Engineering Systems and Environment, University of Virginia, Charlottesville, VA, 22903, USA. Email: heydarian@virginia.edu.

* Tianyu Shi is the corresponding author.

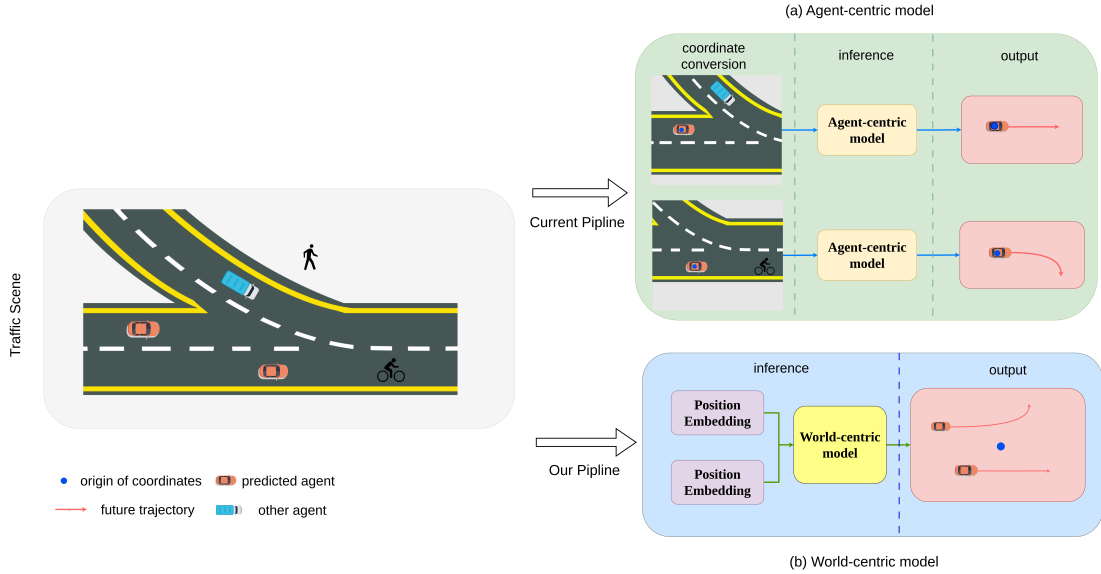


Figure 1: World-centric model and Agent-centric model: (a) The conventional trajectory prediction model is called the “Agent-centric model” and the methods in the Sim Agents leaderboard are based on it. (b) In contrast, our method uses position embedding to replace the cumbersome coordinate transformation; it also implements multi-scenario multi-agent trajectory generation, which significantly improves reasoning efficiency.

one trajectory for each agent per inference time, which can lead to expensive execution latency [31].

In this paper, we introduce an innovative framework for generating traffic scenes tailored to autonomous driving applications, harnessing the complementary capabilities of diffusion models and transformer-based encoder-decoder frameworks. Our proposed framework, named the “World-Centric Diffusion Transformer” (WcDT), optimizes the trajectory generation pipeline from feature extraction to model inference. A distinctive feature of WcDT is its ability to concurrently generate coherent and joint future movements for a comprehensive set of agents, such as vehicles, bicycles, and pedestrians, within a single inferential procedure. The primary contributions of this research can be highlighted as follows:

- We introduce a novel paradigm for traffic scene generation that enables the simultaneous generation of consistent and joint future movements for all involved agents in a single inference pass.
- We construct a Diffusion-Transformer module that significantly enriches scene diversity and the stochasticity of agent behaviors. This architecture stands out for its efficiency and its holistic integration of the world state.
- Our model sets a new benchmark for realism and diversity in trajectory generation, as evidenced by its performance on the open-sourced traffic generation dataset. The developed software and demos are available in our open-source repository¹.

The remainder of this paper is organized as follows. Section II provides a comprehensive literature review on existing work for traffic scene generation. The problem formulation and the proposed WcDT framework are introduced in Section III

whereas experiments, results, and discussions are presented in Section IV. Lastly, in Section V, we conclude the paper, summarize our contributions, and suggest potential insights for future research.

II. RELATED WORK

Traffic simulators play a crucial role in evaluating the efficiency and effectiveness of ADS, which can be broadly classified into rule-based and learning-based approaches. Rule-based approaches excel in accurately capturing high-level traffic characteristics through the direct encoding of traffic rules [32]. Despite their precision in adhering to established regulations, these methods tend to exhibit a lack of flexibility, often leading to simulations that might not fully capture the complexity and variability of real-world driving behaviors [13], [19]. In contrast, learning-based approaches enhance the realism of traffic simulations by analyzing and applying patterns derived from extensive datasets of actual driving trajectories [13], offering a more nuanced and adaptable representation of vehicular dynamics. Therefore, in this study, we will focus on the learning-based approaches.

A. Motion prediction-based methods

Recent advancements in traffic scene generation have seen a shift towards employing motion prediction-based methodologies to create multimodal traffic scenarios [16]–[22], which leverage sophisticated algorithms to forecast the movements of various traffic participants, thereby enriching the realism and complexity of simulated environments. For instance, Multi-path++ [17] enhances the trajectory prediction capabilities of its predecessor, Multipath [16], by incorporating a context-aware fusion technique and integrates diverse inputs reflecting

¹<https://github.com/yangchen1997/WcDT>

the current state of the world to generate multimodal trajectories using Gaussian mixture models, leading to more accurate and varied path predictions. Trafficsim [19] capitalizes on recent breakthroughs in motion forecasting by adopting an implicit latent variable model to simulate multi-agent behaviors within traffic systems.

The exploration of transformer-based encoder-decoder architectures for motion prediction underscores a pivotal development in the field [18], [20]–[22]. Specifically, the Scene Transformer [18] introduces a novel approach by utilizing a global coordinate frame to encode the interactions among multiple agents, thereby facilitating the joint prediction of behaviors for all agents involved. Moreover, the Motion Transformer (MTR) [20] emerges as a leading example within the transformer encoder-decoder framework for multimodal motion prediction by concurrently optimizing for global intention localization and local movement refinement, securing the top position on the leaderboards of the Waymo Open Motion Dataset [23] at the time of publication. Building on these advancements, the Multiverse Transformer (MVTA) has emerged as the current top performer in the Waymo Open Sim Agents Challenge (WOSAC). This model introduces innovative training and sampling techniques, alongside a receding horizon prediction mechanism, to further push the boundaries of accuracy and efficiency in motion prediction for autonomous driving applications. Despite these advancements, scene generation requires considering multimodal features of the entire environment (including surrounding agents and maps), whereas trajectory prediction primarily concentrates on the surrounding scene information of the predicted agent. Hence, the key limitation in employing trajectory prediction methods for scene generation lies in the inability to generate actions for all agents based on comprehensive “global” information. Furthermore, unlike our diffusion-based model which can generate varied actions at each inference, trajectory prediction methods cannot spontaneously generate actions.

B. Generative model-based methods

Generative adversarial networks (GANs) [24]–[26] and Variational Auto-Encoders (VAEs) [27], [28] have been explored for generating traffic scenes. For instance, in [24], a conditional generative neural system (CGNS) is proposed for probabilistic trajectory generation to approximate the data distribution. In [28], a conditional VAE is developed to extensively perform multimodal and context-driven generative tasks for high-dimensional traffic scene generation problems. However, these methods often tend to generate unrealistic trajectories as they primarily mirror the distribution of the training data and lack diversity [13]. Additionally, the training process for GANs can be unstable due to adversarial learning [15] and VAEs often have limited expressiveness of the latent space as they often assume a simple Gaussian prior over the latent variables, which can limit the expressiveness of the model.

Recently, diffusion models have emerged as a compelling alternative to GANs and VAEs in the generation of realistic and diverse data [13], [29]. Notably, a classifier-guided

diffusion approach has been innovatively applied in [29] to trajectory data alongside a probabilistic framework tailored for synthesizing behaviors. In [13], a novel conditional diffusion model is introduced for controllable traffic generation (CTG), enabling users to specify desired trajectory properties during test time—such as achieving a specific goal or adhering to speed limits—while ensuring the outcomes remain realistic and physically plausible through dynamic constraints. However, it is important to note that these methodologies are primarily focused on generating behaviors for single agents.

On the other hand, the exploration into multi-agent trajectory generation leveraging diffusion models has subsequently garnered increasing attention [15], [30]. Specifically, SceneDM [15] proposes a novel framework based on diffusion models to generate future motions of all the agents, yielding state-of-the-art results on the Waymo Sim Agents Benchmark. In DJINN [30], a conditioned diffusion model is developed to generatively produce traffic scenarios over the joint states of all agents in the scene. However, a notable limitation of these models is their tendency to predict trajectories for individual agents per inference time. In contrast, our approach is designed to produce joint and coherent future trajectories for all agents simultaneously.

To tackle the above challenges, we integrate diffusion models with transformer-based encoder-decoder architectures, enhancing the efficiency and effectiveness of the traffic scene generation process. This innovative approach leverages the strengths of both technologies to generate more accurate and cohesive multi-agent trajectories. Details of this methodology will be elaborated in the subsequent sections.

III. WCDT FOR TRAFFIC SCENE GENERATION

In this section, we detail our novel WcDT framework, designed to represent and generate complex traffic scenes. First, we illustrate our approach to modeling the intricacies of traffic environments, followed by a comprehensive introduction to our framework and its components.

A. Traffic scene representation

Traffic environments are characterized by multimodal data, including road layouts, traffic signal statuses, historical and predictive agent movements, pedestrian dynamics, and varying environmental conditions [33], [34]. To adeptly encode these diverse elements within our WcDT framework, we utilize a unified approach that effectively captures the essence of traffic scenes, including predicted agents and environmental agents (i.e., world agents). Contrasting with existing methodologies, which require information to be transformed according to the individual perspective or center of each agent [16], Our approach simplifies the encoding process by:

- Transforming the positions of both predicted agents and world agents into a unified Frenet coordinate system, facilitating a standardized representation.
- Representing the historical trajectories of predicted agents through movement statements rather than traditional coordinate vectors, enhancing the clarity and interpretability of data.

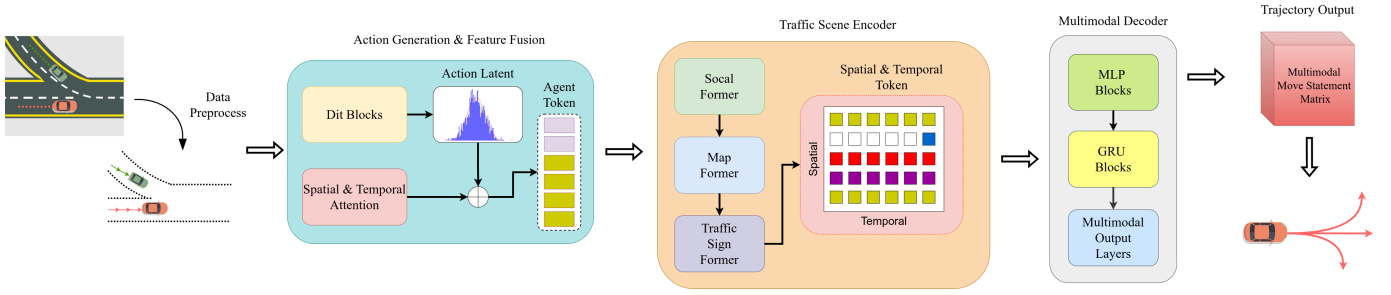


Figure 2: Overview of Scene Encoder, which consists of the following modules: (a) Embedding blocks for encoding the position and features of multimodal scene information; (b) Spatial and temporal attention module for encoding the temporal and spatial information of predicted agents; (c) Multimodal features former for incorporating information from other agents, map points and traffic light features in the traffic scene; (d) Fusion blocks for fusing the previous features and generating trajectories.

Within our WcDT framework, we define key variables for simulating traffic scenarios:

- \mathcal{A}_{all} , \mathcal{A}_p , and \mathcal{A}_w : The counts of all agents, predicted agents, and world agents, respectively.
- \mathcal{T}_h and \mathcal{T}_f : Historical and future prediction time steps.
- \mathcal{L} and \mathcal{P} : The traffic lane lines and specific points on them in the scenarios.
- \mathcal{S}_{tl} : Traffic light states implicitly dictating agent flow.
- \mathcal{D} : Dimensionality of features for representing data.

For different objects in the traffic scenes, we represent them in different formats.

- *Agent move statement and features*: To mitigate the impact of varying agents' positions on historical and future trajectories, we introduce the absolute states to represent the past and prospective states of agents. Specifically, for agent i at time step t , the state s_t is represented as $s_t^i = [(x_t - x_{t-1}), (y_t - y_{t-1}), (\theta_t - \theta_{t-1}), (v_t - v_{t-1})]$. Here, x_t , y_t , θ_t , and v_t represent the longitudinal position, lateral position, heading angle, and velocity at time step t , respectively. The dimensional space for each agent's features is $[\mathcal{A}, \mathcal{T}_h - 1, \mathcal{D}]$.
- *Traffic light feature*: The dataset for traffic lights within each scenario, denoted as $[\mathcal{S}_{tl}, \mathcal{T}_h, \mathcal{D}_t]$, includes the positions and operational statuses of traffic signals across historical intervals. For any given traffic signal point $s_{tl} \in \mathcal{S}_{tl}$, we represent this information through a one-hot encoding of the traffic light signals and the spatial positioning of traffic lights at each historical moment.
- *Map feature*: The map features, denoted as $[1, \mathcal{L}, \mathcal{P}, \mathcal{D}_m]$, include essential lane information within a traffic scenario, such as lane positions and types. Each lane line $l_t \in \mathcal{L}$ at the current time step is characterized by a detailed representation, using one-hot encoding to specify the positions of all points along the lane and to define the lane's type.

Figure 2 shows an overview of our proposed WcDT framework for traffic scene generation, including three major components: action diffusion, scene encoder, and trajectory decoder, which are detailed in the following subsections.

B. Action Diffusion

To enrich the diversity of generated trajectories in our WcDT framework, we encode the agent actions into latent space which increases the uncertainty of agents' actions. The generated latent features are then used as one of the inputs to the scene encoder. Our approach utilizes Denoising Diffusion Probabilistic Models (DDPM) [35] for the encoding of actions. Traditionally, DDPM relies on a convolutional U-Net architecture. However, recent studies, including [36], suggest that the specific inductive biases of U-Net are not essential for diffusion model performance. The advent of transformer networks [37] has revolutionized domain-specific architectures in fields ranging from language and vision to reinforcement learning, showing exceptional scalability with increases in model size, computational power, and data volume. Motivated by these advancements, our work replaces the conventional UNet with transformer modules within the conditional diffusion model framework, i.e., the "Diffusion Transformers" (DiTs) module to significantly boost the performance of our framework [36] and ensure more diverse trajectories for agents in simulated environments.

Figure 3 shows the architecture of the conditional DiT blocks for the action latent encoding. The network takes random noise points, time steps, and historical trajectories of agents as input features and outputs "action latent" to the scene encoder. To refine the DiT network, the DDPM's loss function is meticulously designed to encourage the network to produce an "action latent" that adheres to the kinematic constraints of the agents [35]. This optimization not only aligns with the physical laws governing agent movements but also enhances the variability of their actions due to the inherent unpredictability of the data generated by the diffusion model. The loss function for updating the DiT module is denoted as follows:

$$\mathcal{L}_{diff} = \|\epsilon - \epsilon_\theta(\sqrt{\bar{\alpha}_t}x_0 + \sqrt{1 - \bar{\alpha}_t}\epsilon, t)\|^2. \quad (1)$$

where $\bar{\alpha}_t$ are hyperparameters specified prior to diffusion model training. ϵ_θ is the diffusion model integrated with DiT blocks, and θ is the learnable parameter. ϵ is a set of standard normally distributed random noise points.

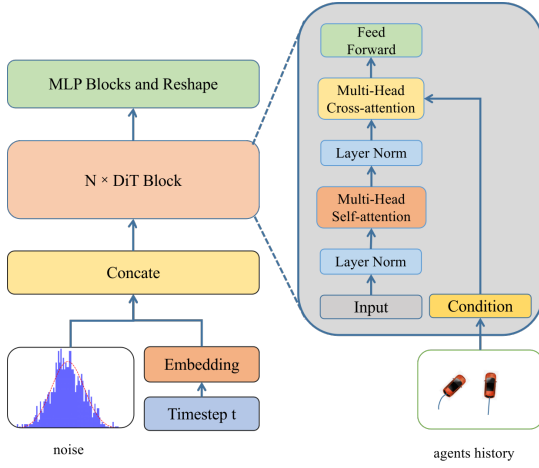


Figure 3: Overview of the developed conditional DiT blocks for action latent encoding: taking random noise points, time steps, and historical trajectories of agents as input features and outputting “action latent” to scene encoder.

C. Scene Encoder

In the traffic scene, various agents may present, including predicted agents (e.g., vehicles, pedestrians, and bicycles), world agents (e.g., other vehicles, pedestrians, and bicycles), map features, and traffic light information. To effectively generate realistic and diverse trajectories, we encode the agents with different *embedding* blocks with different sizes and layers. These blocks globally encode the agent’s characteristics, thereby avoiding the need to convert the coordinate system into a Frenet coordinate system centered around individual agents – a common necessity in the existing trajectory prediction models. The Pose-Embedding encodes all positional attributes p_i into a unified one-dimensional matrix, while the Feature-Embedding translates the agent’s features (including height, width, and type, the latter in one-hot encoding format) into a one-dimensional matrix as well. For a given predicted agent i :

$$E_p = \phi_p[x_i, y_i], \quad (2)$$

where ϕ_p represents a linear transformation layer, and E_p denotes the positional embedding result. The feature embedding outcome E_f is denoted as:

$$E_f = \phi_f[f_w, f_h, f_{type}], \quad (3)$$

where ϕ_f indicates a linear transformation layer, with f_w and f_h representing the agent’s width and height, respectively, and f_{type} specifying the agent’s type after conversion to a one-hot encoded format. To synthesize these embedding into a comprehensive agent representation, we apply:

$$E_A = \text{ReLU}(\text{LayerNorm}(\text{Concat}(E_p, E_f))) \quad (4)$$

where E_A is the agent’s final embedded representation, achieved by concatenating the positional and feature embeddings, followed by normalization and the application of the ReLU activation function. This process ensures a robust and nuanced representation of each agent within the WcDT

framework, enhancing the model’s ability to accurately capture traffic dynamics.

To accurately represent traffic scenarios, the encoding process also encompasses world agent A_w , map A_m , and traffic light A_l features, ensuring these elements are seamlessly integrated. First, an encoding layer processes each raw feature to yield embedded representations, e.g., E_w , E_m , and E_l . Subsequently, these representations are refined through a series of advanced neural network blocks, including a multi-head self-attention block for detailed feature analysis, a cross-attention block for inter-feature relationships, and fully connected layers designed for the advanced extraction and integration of features. Here attention layers are employed instead of traditional CNNs due to their ability to dynamically focus on relevant input features, efficiently capture long-range dependencies, and offer enhanced interpretability and flexibility across diverse inputs. The multi-head self-attention layers for the world agent encoding are denoted as:

$$q_{A_p} = W^{Q \times h} E_p, k_{A_p} = W^{K \times h} E_p, v_{A_p} = W^{V \times h} E_p, \\ \alpha_{A_p} = \text{Softmax} \left(\frac{q_{A_p}^T k_{A_p}}{\sqrt{d_k}} \right), \quad (5)$$

$$\text{Self}_{A_p} = \alpha_{A_p} v_{A_p}, \quad (6)$$

where W^Q , W^K , W^V are learnable parameters and E_{A_p} is the result of the predicted agent after the embedding block. After the self-attention layer, the cross-attention encoding is denoted as:

$$q_{A_p} = W^{Q \times h} E_{A_p}, k_{A_p} = W^{K \times h} E_{A_w}, v_{A_p} = W^{V \times h} E_{A_w}, \\ \alpha_{A_o} = \text{Softmax} \left(\frac{q_{A_p}^T k_{A_o}}{\sqrt{d_k}} \right), \quad (7)$$

$$\text{Cross}_{A_p} = \alpha_{A_p} v_{A_p}, \quad (8)$$

where W^Q , W^K , W^V are learnable parameters.

Cross Attention in Map Former:

$$q_{A_p} = W^{Q \times h} E_{A_p}, k_m = W^{K \times h} E_m, v_m = W^{V \times h} E_m, \\ \alpha_m = \text{Softmax} \left(\frac{q_{A_p}^T k_m}{\sqrt{d_k}} \right), \quad (9)$$

$$\text{Cross}_m = \alpha_{A_p} v_m, \quad (10)$$

where W^Q , W^K , W^V are learnable parameters.

Cross Attention in Traffic Light Former:

$$q_{A_p} = W^{Q \times h} E_{A_p}, k_l = W^{K \times h} E_l, v_l = W^{V \times h} E_l, \\ \alpha_m = \text{Softmax} \left(\frac{q_{A_p}^T k_l}{\sqrt{d_k}} \right), \quad (11)$$

$$\text{Cross}_l = \alpha_{A_p} v_l, \quad (12)$$

where W^Q , W^K , and W^V are learnable parameters.

Spatial and Temporal Fusion. To effectively capture the dynamic and complex nature of traffic scenarios, we propose a Temporal Spatial Fusion Attention layer to distill the temporal and spatial characteristics of predicted agents’ movements and integrate multi-modal data, including predicted agents, world agents, map configurations, and traffic signals within traffic

environments. The ADV’s features are augmented with the “action latent” generated from Eq. 4 for enhanced movement descriptions. To distill critical insights from the spatial-temporal data, multi-head self-attention blocks are employed. For the broader multi-modal context of traffic scenes, these blocks identify key spatial and temporal details, which are then restructured through MLP blocks to fit the trajectory decoder’s requirements, ensuring a thorough and accurate understanding of traffic dynamics.

D. Trajectory Decoder

The trajectory decoder plays a crucial role in decoding the fused traffic features into the future trajectories of agents. In this paper, the decoder is comprised of GRU blocks [38] and MLP blocks, specifically tailored to handle the temporal variations in agent movements. Inspired by [39] on multimodal trajectory prediction, which underscores its adaptability to agents exhibiting a range of behaviors over time, we introduce a multimodal output mechanism to effectively cater to agents with varied actions. To mitigate the impact of agents’ differing initial positions on the outcomes, our model outputs include agents’ move statements alongside their likelihoods. The trajectory for model \mathcal{M} is formulated as:

$$\text{Traj}_a^m = \text{Pos}_a + \sum_{i=t}^{T_f} [\Delta x_m, \Delta y_m, \Delta \theta_m], \quad (13)$$

where Pos_a is the agent’s position at the current time step, and Traj_a^m represents the projected future trajectory points for agents in model \mathcal{M} . These points are calculated from the agent’s initial position Pos_a , adjusted by the incremental displacement $[\Delta x_m, \Delta y_m, \Delta \theta_m]$ for each subsequent time step t . The speed is determined as:

$$\text{Speed}_a^m = \frac{[\Delta x_m, \Delta y_m]}{\Delta t}, \quad (14)$$

with the speed Speed_a^m being derived from the displacement $[\Delta x_m, \Delta y_m]$ over the time interval Δt . This approach, based on kinematic rules, calculates the agents’ move statements, resulting in a multi-modal trajectory output formatted as $[x_a^m, y_a^m, \theta_a^m, v_a^m]$.

E. Loss functions

In this paper, the objective is to guarantee that the generated trajectories adhere to scene constraints and simultaneously preserve trajectory diversity. The trajectory from the multimodal set with the minimal loss is selected, and its deviation from the ground truth is quantified using the Huber loss [40] as follows.

$$\mathcal{L}_{reg} = \text{Huber}(\text{Traj}_p, \text{Traj}_{gt}), \quad (15)$$

where Traj_p represents the predicted trajectory for the modality with the lowest loss, and Traj_{gt} is the ground truth trajectory.

In addition, we introduce classification loss, which helps the model to find out the closest modality to the ground truth. During training, we take the modality with the smallest AED as the truth of classification, the classification loss \mathcal{L}_{cls} is formulated as:

$$\mathcal{L}_{cls} = - \sum_{i=1}^M y_i \log(p_i), \quad (16)$$

Hence, the overall loss function employed is the aggregate of diffusion loss, regression loss, and classification loss as:

$$\mathcal{L}_{total} = \mathcal{L}_{diff} + \mathcal{L}_{reg} + \mathcal{L}_{cls}. \quad (17)$$

where \mathcal{L}_{diff} is the standard diffusion model loss function which is computed as the L2 loss of the predicted noise and the original noise.

IV. EXPERIMENTS AND RESULT ANALYSIS

In this section, we evaluate the performance of our WcDT model on a public traffic dataset, comparing it against leading methods and conducting ablation studies to highlight its effectiveness in traffic scene generation for autonomous driving simulations.

A. Experimental Setup

Dataset. We develop and assess our traffic scene generation model using the Waymo Motion Prediction dataset [23], which offers detailed motion trajectories of agents and high-definition map data. The dataset includes 576,012 authentic driving scenarios and is divided into 486,995 scenarios for training, 44,097 for validation, and 44,920 for testing [41]. Each traffic scenario is captured for 9 seconds, with sequences sampled at a frequency of 10 Hz. In testing scenarios, only the initial 1-second segment of the trajectory is made publicly accessible and the developed algorithms are expected to accurately generate the motion trajectories of agents for the subsequent 8 seconds, based on this limited initial data.

Metrics. To assess the realism and diversity of the trajectories generated by our model, we employ the evaluation metrics aligned with those established in the literature [19], [42], [43], and utilize the Sim Agents Challenge metrics [42]. These metrics allow us to measure the alignment between our generated trajectories and the ground truth, focusing on three essential aspects: kinematic metrics, object interaction metrics, and map-based metrics. The detailed criteria of these evaluations are presented in Appendix A.

In this study, we refer to the Sim Agents Challenge metrics, which assess the similarity between generated trajectories and ground truth along three dimensions: kinematic metrics, object interaction metrics, and map-based metrics [19], [42], [43], as shown in Section A.1 of the Appendix. We adopt the approximate negative log-likelihood (NLL) to evaluate similarity, the NLL we wish to minimize the following equation:

$$NLL^* = - \frac{1}{|\mathcal{D}|} \sum_{i=0}^{|\mathcal{D}|} \text{Log} q^{world}(o_{\geq t,i} | o_{< t,i}), \quad (18)$$

where $o_{< t,i}$ denotes historical observations, including map observations, traffic light observations, and agents’ historical observations and $o_{\geq t,i}$ denotes future observations. where q^{world} is the “world model”.

Implementation Details. We train our model over 128 epochs utilizing two NVIDIA A100 GPUs, employing the Adam optimizer for optimization purposes [44]. The batch size, initial learning rate, diffusion time steps, and dropout rate are set as 128, 2×10^{-4} , 100, and 0.1, respectively. To further enhance the stability of the training process, a cosine annealing scheduler [45] is employed to methodically reduce the learning rate as training progresses, ensuring gradual convergence to optimal solutions. The architecture of the model is composed of several components (see Section III): the backbone features an Action Diffusion mechanism with 2 DiT blocks; the Scene Understand Encoder, which includes 4 Other Agent Former blocks, 4 Map Former blocks, and 2 Traffic Light Former blocks; and the Trajectory Decoder, which is equipped with 2 MLP blocks. Both Multi-Head Self-Attention and Multi-Head Cross-Attention mechanisms within the Scene Encoder utilized an identical configuration in terms of the number of heads and hidden units. To assess the impact of model scale on its overall performance, our experiments encompass two distinct model variants: the smaller WcDT-64, featuring 8 attention heads and 64 hidden units, and the more expansive WcDT-128, with 8 attention heads and 128 hidden units. The current location of the self-driving vehicle is designated as the coordinate origin for the traffic scenario to ensure a consistent reference point for all trajectory predictions.

B. Comparison with state-of-the-art methods

In this subsection, we conduct a comprehensive comparison of our proposed method against a range of state-of-the-art benchmarks that were submitted to the Sim Agent Challenge² [42], including Random Agent [42], Constant Velocity [42], MTR+++ [46], WayFormer [33], MULTIPATH++ [17], MVTA [22], and MVTE [22]. Among these competitors, MVTE [22], MVTA [22], and MTR+++ [46] are highlighted for their exceptional performance, demonstrating advanced capabilities in generating realistic and feasible motion trajectories for autonomous vehicles within simulated environments.

Table I shows the evaluation results on the testing datasets for all considered algorithms. Notably, the Random Agent method [42] which generates trajectories randomly, exhibits the worst performance, achieving the lowest composite metric score of 0.163. This metric, aggregating the metrics across multiple features (similarity metrics, kinematic metrics, object interaction metrics, and map-based metrics), forms the overall evaluation for the overall ranking. Conversely, the Constant Velocity Agent [42] which predicts future trajectories based on the last known heading and speed from the given context or historical data, performs marginally better. Despite its failure to excel in the generative tasks, this method records a slightly higher composite metric of 0.238, alongside improved ADE and MinADE scores compared to the Random Agent. This enhancement is attributed to its utilization of kinematic information as input, underscoring the value of incorporating basic physical principles into trajectory prediction models.

²Sim Agent Leaderboard at 02-04-2024: <https://waymo.com/open/challenges/2023/sim-agents/>

Markedly, the MVTE algorithm [22] stands out with the highest composite metric at 0.517, indicating the most robust performance among the evaluated methods. Our proposed model, WcDT, closely trails with a composite metric of 0.511, yet surpasses MVTE in specific areas such as Linear Speed, Linear Acceleration, Angle Speed, Distance to Object, and Distance to Road Edge metrics, in addition to achieving better MinADE scores. This nuanced performance underscores WcDT’s specialized capabilities in rendering precise and contextually appropriate trajectory predictions, evidencing its advanced integration and interpretation of dynamic traffic environment variables.

C. Impact of the number of agents

In this subsection, we evaluate how the number of agents within a scenario affects trajectory generation, specifically focusing on the ADE metric. Figure 4 illustrates the distribution of agents in 10,000 random samples from the testing dataset, revealing that scenarios containing between 2 to 6 agents constitute most of the dataset. Additionally, Figure 4 highlights a trend where an increase in the number of agents correlates with a decline in model performance. This observation suggests that higher traffic densities, represented by more agents, introduce complexities in interactions that challenge the model’s generation accuracy.

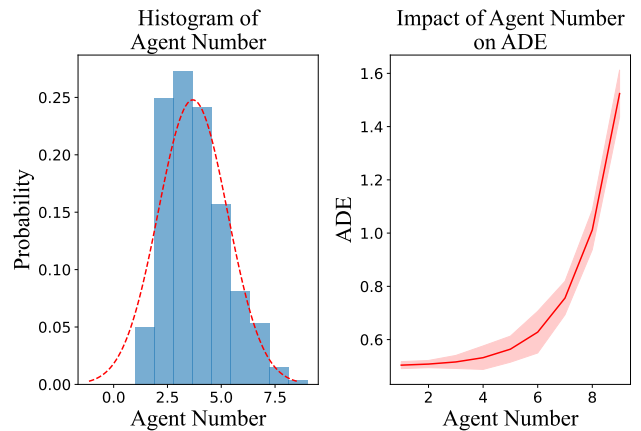


Figure 4: Histogram of the number of agents and the effect of the number of agents on ADE.

D. Ablation studies on diffusion model

In this subsection, we assess the impact of the action latent encoding module when fed with random noise inputs, the efficacy of the Unet network structure, and the performance of our custom-designed DiT block. The results, presented in Table II, highlight that the DiT module outperforms others in achieving the lowest ADE and minADE scores, alongside the highest composite score. This indicates that the diffusion model, underpinned by the DiT module, substantially enhances the diversity of agent actions while maintaining trajectory plausibility.

Method	Linear Speed	Linear Accel	Ang Speed	Ang Accel	Dist to Obj	Collision	TTC	Dist to Road Edge	Offroad	Composite Metric	ADE	MinADE
Random Agent [42]	0.002	0.044	0.074	0.120	0.000	0.006	0.734	0.178	0.325	0.163	50.740	50.707
Constant Velocity [42]	0.074	0.058	0.019	0.035	0.208	0.202	0.737	0.454	0.325	0.238	7.924	7.924
MTR+++ [46]	0.412	0.107	0.484	0.437	0.346	0.414	0.797	0.654	0.577	0.470	2.129	1.682
WayFormer [33]	0.408	0.127	0.473	0.437	0.358	0.403	0.810	0.645	0.589	0.472	2.588	1.694
MULTIPATH++ [17]	0.432	0.230	0.515	0.452	0.344	0.420	0.813	0.639	0.583	0.489	5.308	2.052
MVTA [22]	0.437	0.220	0.533	0.481	0.373	0.436	0.830	0.654	0.629	0.509	3.938	1.870
MVTE [22]	0.443	0.222	0.535	0.481	0.382	0.451	0.832	0.664	0.641	0.517	3.873	1.677
WcDT (Ours)	0.445	0.248	0.538	0.460	0.387	0.403	0.792	0.668	0.608	0.511	4.563	1.669

Table I: Quantitative results on the Sim Agents Leaderboard: We refer to the Sim Agents Challenge metrics, which contain two types of metrics: similarity metrics (10 metrics on the left) and distance error metrics (ADE and MinADE). There are three types of similarity metrics, kinematic metrics, object interaction metrics, and map-based metrics and the composite metric combines the above metrics. Higher values of these metrics represent better performance. ADE and MinADE are commonly used in trajectory prediction, with lower values indicating closer proximity to the ground truth.

Random Noise	Unet	Dit Blocks	ADE↓	minADE↓	Composite Metric↑
✓			5.950	2.715	0.326
	✓		5.184	1.907	0.480
		✓	4.563	1.669	0.511

Table II: Ablation Study on Diffusion Model: We evaluate the contribution of the diffusion model and compare the impact on the results of Dit Blocks and Unet as the backbone of the diffusion model.

E. Ablation studies on traffic scene encoder

In this subsection, we evaluate the traffic scene encoder’s structure by adding or removing its components, including the Spatial & Temporal Attention module, Other Agent Former, HD Map Former, and Traffic Light Former. ADE and MinADE metrics are employed to assess how well the generated trajectories match the ground truth.

Table III presents the evaluation results, highlighting the HD Map Former as the crucial component for accurate trajectory generation. The model records its worst ADE and MinADE performance in the absence of this module, indicating its key role in ensuring generated trajectories adhere to lane constraints. Similarly, the Spatial & Temporal Attention blocks are critical, markedly improving the scene encoder’s understanding of traffic scenarios. Their absence results in sub-optimal ADE and MinADE scores of 4.803 and 1.973, respectively. The Traffic Light Former also emerges as essential, its absence reflecting negatively on trajectory accuracy to a degree comparable to missing the Spatial & Temporal Attention block. Additionally, the Other Agent Former proves vital in incorporating the historical motion of nearby agents, crucial for generating safe trajectories. Incorporating all these modules, our traffic scene encoder, WcDT, achieves the best performance, reflected in the lowest ADE and MinADE, demonstrating the effectiveness of our comprehensive approach in encoding the surrounding environments.

F. Ablation studies on trajectory decoder

In this subsection, we assess the architecture of the trajectory decoder, focusing on the contributions of GRU (Gated Recurrent Unit) blocks, MLP (Multi-Layer Perceptron) blocks, and various network configurations. This evaluation aims to

Spatial & Temporal Attention	Other Agent Former	HD Map Former	Traffic Light Former	ADE↓	minADE↓
	✓	✓	✓	4.803	1.973
✓		✓	✓	4.591	1.883
✓	✓		✓	5.083	2.130
✓		✓		4.734	1.865
✓	✓	✓	✓	4.563	1.669

Table III: Ablation Study on the Components of Scene-Encoder: We evaluate the importance of each module by adding and removing a module from the scene encoder, and then use ADE and minADE to evaluate model performance.

determine how each component and setup influences the decoder’s ability to accurately predict future trajectories, highlighting the significance of these elements in enhancing the model’s performance.

Table IV shows the evaluation results, underlining the critical role of MLP layers in the trajectory decoder’s performance. The absence of MLP blocks leads to significantly poorer results, with the model yielding its highest ADE and MinADE scores of 5.290 and 2.475, respectively. This decline in performance is attributed to the MLP blocks’ fundamental role in refining the predictive capabilities of the decoder and processing and integrating complex features extracted from the input data. Furthermore, the GRU blocks are underscored as vital for enabling the decoder to effectively leverage historical information, further contributing to the accurate prediction of future trajectories. Incorporating both MLP and GRU blocks, our WcDT model achieves optimal results, demonstrating superior trajectory generation with the lowest ADE and MinADE scores.

MLP Blocks	GRU Blocks	Dimension	ADE↓	minADE↓
	✓	64	5.438	2.532
	✓	128	5.290	2.475
✓		64	4.570	1.805
✓		128	4.568	1.780
✓	✓	64	4.565	1.735
✓	✓	128	4.563	1.669

Table IV: Ablation Study on the Trajectory Decoder: We evaluated the impact of different components in the trajectory decoder on the performance of the model. Moreover, we also evaluated the effect of the dimensionality of the hidden units in the trajectory decoder on ADE and minADE.

G. Ablation studies on network structures

In this subsection, we examine how varying the number of modalities and attention heads influences the quality of generated trajectories across different model scales. Table V illustrates that the WcDT-128 model consistently outperforms the WcDT-64 variant, suggesting that models equipped with more attention layers tend to offer improved performance, highlighting the beneficial impact of increased model complexity on the precision and reliability of trajectory predictions. Furthermore, comparing the single-modality with the multi-modality configuration in the WcDT-64 model reveals that the latter achieves superior performance. This is because of the multi-modality trajectory decoder’s ability to leverage a broader spectrum of information, enabling a more nuanced and comprehensive understanding of the driving environment, thereby facilitating more accurate trajectory generation.

Method	Multimodal	Attention Block Heads	ADE↓	minADE↓
WcDT-64	1	8	5.331	2.864
WcDT-64	10	8	5.082	2.548
WcDT-64	10	16	4.997	2.470
WcDT-64	30	16	4.872	1.962
WcDT-128	10	8	4.662	1.781
WcDT-128	30	16	4.563	1.669

Table V: Impact of multimodal trajectory decoders and dimension of attention blocks on scene generation performance

V. CONCLUSION

In this paper, a new traffic scene generation framework was proposed with an optimized trajectory generation process from feature extraction to model inference with advanced Diffusion with Transformer (DiT) blocks. The latent features, historical trajectories, HD map features, and historical traffic signal information were fused with various transformer-based encoders equipped with powerful attention modules. A novel trajectory decoder was further proposed to generate multimodal future trajectories. The experimental results showed that the proposed approach set a new benchmark for realism and diversity in trajectory generation, as evidenced by the open-sourced traffic generation dataset. Future work will focus on proposing more robust algorithms for accommodating complex urban traffic scenarios and more predicted agents.

APPENDIX

A. Sim Agents Challenge metrics

In this paper, the Sim Agents Challenge metrics [42], including kinematic metrics, object interaction metrics, and map-based metrics, are employed for evaluating the generated trajectories.

The kinematic metrics utilized to assess the similarity between the kinematic features of the generated trajectories and the ground truth encompass linear speed, linear acceleration, angular speed, and angular acceleration. These metrics are crucial for evaluating the dynamic aspects of the trajectories:

- **Linear Speed:** Calculated using the 3-dimensional positional data between successive time steps, the linear speed metric is defined as:

$$v_l^t = \left\| \frac{Pos_t - Pos_{t-1}}{\Delta t} \right\|_2, \quad (19)$$

where Pos_t and Pos_{t-1} represent the positions at the current and previous time steps, respectively, and Δt is the time interval between these steps.

- **Linear Acceleration:** This metric quantifies the rate of change in linear speed over time and is expressed as:

$$a_l^t = \frac{v_l^t - v_l^{t-1}}{\Delta t}, \quad (20)$$

highlighting how quickly an agent accelerates or decelerates in the linear direction.

- **Angular Speed:** Reflecting the rate at which an agent changes its orientation, angular speed is calculated by:

$$v_\theta^t = \frac{|\theta_t - \theta_{t-1}|}{\Delta t}, \quad (21)$$

indicating how quickly an agent alters its heading between two-time steps.

- **Angular Acceleration:** This metric determines the change in angular speed over time, given by:

$$a_\theta^t = \frac{v_\theta^t - v_\theta^{t-1}}{\Delta t}. \quad (22)$$

measuring the acceleration in an agent’s rotational movement.

The object interaction metrics serve to assess the similarity of object interaction features between the generated trajectories and the ground truth, focusing on how agents navigate and maintain safety within their environment. These metrics include Time-to-Collision (TTC) and Distance to Nearest Object, which are crucial for evaluating spatial awareness and collision avoidance capabilities:

- **Time-to-collision(TTC):** This metric calculates the time remaining (in seconds) before a potential collision occurs between the current agent and any agent ahead of it on its current trajectory. TTC is a critical safety metric, indicating the urgency of taking evasive action to prevent a collision [47].
- **Distance to Nearest Object:** This metric measures the closest proximity (in meters) of an agent to any other object or agent within the traffic scene. It provides a quantitative assessment of spatial positioning and is essential for evaluating how well the model predicts safe distances between entities to avoid crashes or unsafe interactions.

Map-based metrics play a crucial role in evaluating the interaction between generated trajectories and the road environment, comparing these interactions against the ground truth. These metrics focus on road adherence and the maintenance of safe boundaries, including road departures and distance to road edge:

- **Road Departures:** This metric assesses if, and potentially when, an agent veers off the designated roadway in future time steps. It’s critical for determining the model’s ability to generate trajectories that adhere to road boundaries and maintain lane discipline.

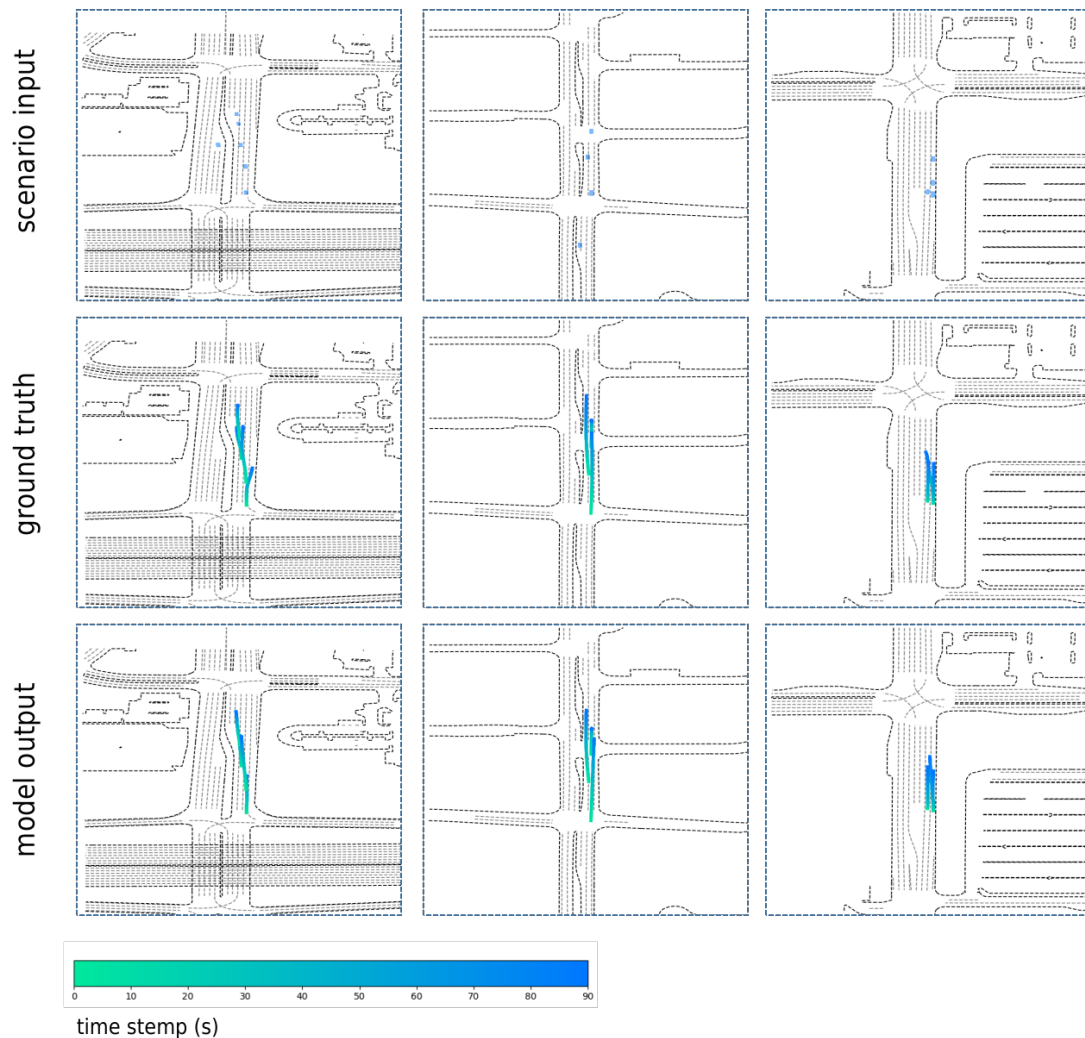


Figure 5: Visualization results of the ground truth and WTSGM-generated trajectories in cruise scenarios.

- Distance to Road Edge:** Measures the shortest Euclidean distance (in meters) from the agent to the nearest edge of the road within the traffic scenario. This metric provides insight into the spatial positioning of the agent relative to the road infrastructure, evaluating the model's capability to keep agents within safe proximity to the roadway and prevent off-road excursions.

B. Visualization Results

Figures 5 and 6 provide visual representations of the generated trajectories for randomly sampled scenarios from the Waymo dataset. The input for these scenarios includes map features, depicted as black dotted lines, and the initial 1-second trajectories of various agents, illustrated with dots. To distinguish between the trajectories of different agents, each is represented by a unique color. Notably, the color intensity of these trajectories deepens progressively with time, providing a visual cue to the temporal progression of each agent's movement.

Figure 5 presents selected scenarios that demonstrate lane-changing maneuvers, showing the capability of our proposed

approach to generate both diverse and accurate trajectories in comparison to ground truth for scenarios necessitating dynamic driving maneuvers. This visualization underscores the model's proficiency in accurately predicting and representing the complex behaviors associated with lane changes, emphasizing its effectiveness in handling intricate driving situations. Meanwhile, Figure 6 shows the model's performance in more complex traffic scenarios involving intersections, where our model impressively achieves high accuracy in trajectory generation, further demonstrating its robustness and adaptability to varied and challenging driving environments.

REFERENCES

- [1] Y. Huang, J. Du, Z. Yang, Z. Zhou, L. Zhang, and H. Chen, "A survey on trajectory-prediction methods for autonomous driving," *IEEE Transactions on Intelligent Vehicles*, vol. 7, no. 3, pp. 652–674, 2022.
- [2] S. Teng, X. Hu, P. Deng, B. Li, Y. Li, Y. Ai, D. Yang, L. Li, Z. Xuanyuan, F. Zhu *et al.*, "Motion planning for autonomous driving: The state of the art and future perspectives," *IEEE Transactions on Intelligent Vehicles*, 2023.
- [3] B. Paden, M. Čáp, S. Z. Yong, D. Yershov, and E. Frazzoli, "A survey of motion planning and control techniques for self-driving urban vehicles," *IEEE Transactions on intelligent vehicles*, vol. 1, no. 1, pp. 33–55, 2016.

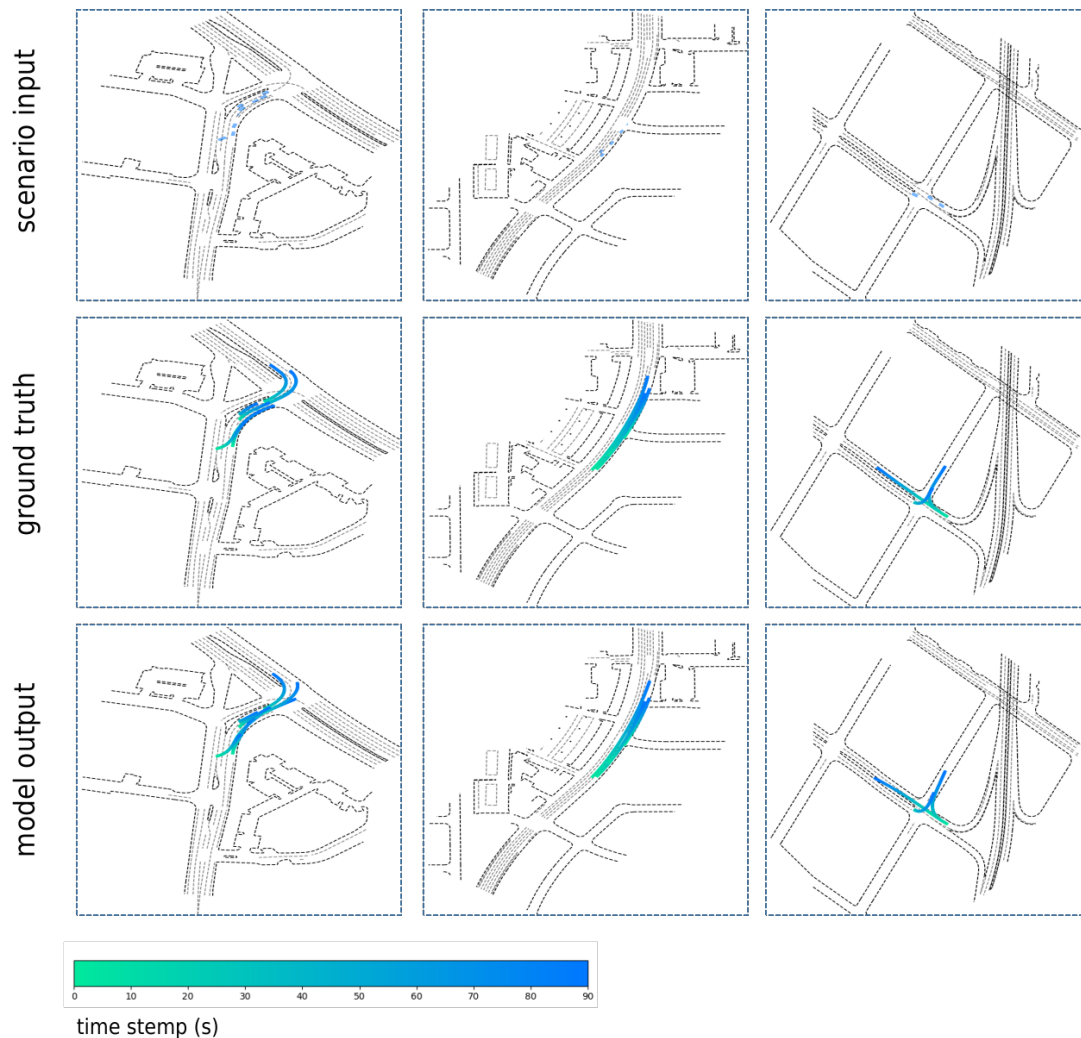


Figure 6: Visualization results of the ground truth and WTSGM-generated trajectories in intersection scenarios.

- [4] D. Chen, K. Zhang, Y. Wang, X. Yin, Z. Li, and D. Filev, "Communication-efficient decentralized multi-agent reinforcement learning for cooperative adaptive cruise control," *IEEE Transactions on Intelligent Vehicles*, 2024.
- [5] L. Chen, Y. Li, C. Huang, B. Li, Y. Xing, D. Tian, L. Li, Z. Hu, X. Na, Z. Li *et al.*, "Milestones in autonomous driving and intelligent vehicles: Survey of surveys," *IEEE Transactions on Intelligent Vehicles*, vol. 8, no. 2, pp. 1046–1056, 2022.
- [6] W. Liu, M. Hua, Z. Deng, Z. Meng, Y. Huang, C. Hu, S. Song, L. Gao, C. Liu, B. Shuai *et al.*, "A systematic survey of control techniques and applications in connected and automated vehicles," *IEEE Internet of Things Journal*, 2023.
- [7] S. Ge, Y. Xie, K. Liu, Z. Ding, E. Hu, L. Chen, and F.-Y. Wang, "The use of intelligent vehicles and artificial intelligence in mining operations: Ethics, responsibility, and sustainability," *IEEE Transactions on Intelligent Vehicles*, vol. 8, no. 2, pp. 1021–1024, 2023.
- [8] M. O’Kelly, A. Sinha, H. Namkoong, R. Tedrake, and J. C. Duchi, "Scalable end-to-end autonomous vehicle testing via rare-event simulation," *Advances in neural information processing systems*, vol. 31, 2018.
- [9] X. Hu, S. Li, T. Huang, B. Tang, R. Huai, and L. Chen, "How simulation helps autonomous driving: A survey of sim2real, digital twins, and parallel intelligence," *IEEE Transactions on Intelligent Vehicles*, 2023.
- [10] S. Grollius, M. Ligges, J. Ruskowski, and A. Grabmaier, "Concept of an automotive lidar target simulator for direct time-of-flight lidar," *IEEE Transactions on Intelligent Vehicles*, 2021.
- [11] E. Weiss and J. C. Gerdes, "High speed emulation in a vehicle-in-the-loop driving simulator," *IEEE Transactions on Intelligent Vehicles*, vol. 8, no. 2, pp. 1826–1836, 2022.
- [12] C. Brogle, C. Zhang, K. L. Lim, and T. Bräunl, "Hardware-in-the-loop autonomous driving simulation without real-time constraints," *IEEE Transactions on Intelligent Vehicles*, vol. 4, no. 3, pp. 375–384, 2019.
- [13] Z. Zhong, D. Rempe, D. Xu, Y. Chen, S. Veer, T. Che, B. Ray, and M. Pavone, "Guided conditional diffusion for controllable traffic simulation," in *2023 IEEE International Conference on Robotics and Automation (ICRA)*. IEEE, 2023, pp. 3560–3566.
- [14] M. Treiber, A. Hennecke, and D. Helbing, "Congested traffic states in empirical observations and microscopic simulations," *Physical review E*, vol. 62, no. 2, p. 1805, 2000.
- [15] Z. Guo, X. Gao, J. Zhou, X. Cai, and B. Shi, "Scenedm: Scene-level multi-agent trajectory generation with consistent diffusion models," *arXiv preprint arXiv:2311.15736*, 2023.
- [16] Y. Chai, B. Sapp, M. Bansal, and D. Anguelov, "Multipath: Multiple probabilistic anchor trajectory hypotheses for behavior prediction," *arXiv preprint arXiv:1910.05449*, 2019.
- [17] B. Varadarajan, A. Hefny, A. Srivastava, K. S. Refaat, N. Nayakanti, A. Comman, K. Chen, B. Douillard, C. P. Lam, D. Anguelov *et al.*, "Multipath++: Efficient information fusion and trajectory aggregation for behavior prediction," in *2022 International Conference on Robotics and Automation (ICRA)*. IEEE, 2022, pp. 7814–7821.
- [18] J. Ngiam, B. Caine, V. Vasudevan, Z. Zhang, H.-T. L. Chiang, J. Ling, R. Roelofs, A. Bewley, C. Liu, A. Venugopal *et al.*, "Scene transformer: A unified architecture for predicting multiple agent trajectories," *arXiv preprint arXiv:2106.08417*, 2021.
- [19] S. Suo, S. Regalado, S. Casas, and R. Urtasun, "TrafficSim: Learning to simulate realistic multi-agent behaviors," *arXiv preprint arXiv:2101.06557*, 2021.
- [20] S. Shi, L. Jiang, D. Dai, and B. Schiele, "Motion transformer with

- global intention localization and local movement refinement,” *Advances in Neural Information Processing Systems*, 2022.
- [21] —, “Mtr++: Multi-agent motion prediction with symmetric scene modeling and guided intention querying,” *IEEE Transactions on Pattern Analysis and Machine Intelligence*, 2024.
- [22] Y. Wang, T. Zhao, and F. Yi, “Multiverse transformer: 1st place solution for waymo open sim agents challenge 2023,” *arXiv preprint arXiv:2306.11868*, 2023.
- [23] Z. Sun, J. Wang, Y. Chen, J. Xu, X. Zhang, Y. Li, Y. Zhang, Z. Liu, J. Guo, T. Huang *et al.*, “Large scale interactive motion forecasting for autonomous driving: The waymo open motion dataset,” in *Proceedings of the IEEE/CVF International Conference on Computer Vision*, 2021, pp. 11 271–11 281.
- [24] J. Li, H. Ma, and M. Tomizuka, “Conditional generative neural system for probabilistic trajectory prediction,” in *2019 IEEE/RSJ International Conference on Intelligent Robots and Systems (IROS)*. IEEE, 2019, pp. 6150–6156.
- [25] S. Choi, J. Kim, and H. Yeo, “Trajgail: Generating urban vehicle trajectories using generative adversarial imitation learning,” *Transportation Research Part C: Emerging Technologies*, vol. 128, p. 103091, 2021.
- [26] R. Bhattacharyya, B. Wulfe, D. J. Phillips, A. Kuefler, J. Morton, R. Senanayake, and M. J. Kochenderfer, “Modeling human driving behavior through generative adversarial imitation learning,” *IEEE Transactions on Intelligent Transportation Systems*, vol. 24, no. 3, pp. 2874–2887, 2022.
- [27] W. Ding, W. Wang, and D. Zhao, “Multi-vehicle trajectories generation for vehicle-to-vehicle encounters,” in *2019 IEEE International Conference on Robotics and Automation (ICRA)*, 2019.
- [28] G. Oh and H. Peng, “Cvae-h: Conditionalizing variational autoencoders via hypernetworks and trajectory forecasting for autonomous driving,” *arXiv preprint arXiv:2201.09874*, 2022.
- [29] M. Janner, Y. Du, J. B. Tenenbaum, and S. Levine, “Planning with diffusion for flexible behavior synthesis,” *arXiv preprint arXiv:2205.09991*, 2022.
- [30] M. Niedoba, J. W. Lavington, Y. Liu, V. Lioutas, J. Sefas, X. Liang, D. Green, S. Dabiri, B. Zwartsenberg, A. Scibior *et al.*, “A diffusion-model of joint interactive navigation,” *arXiv preprint arXiv:2309.12508*, 2023.
- [31] M. Liang, B. Yang, R. Hu, Y. Chen, R. Liao, S. Feng, and R. Urtasun, “Learning lane graph representations for motion forecasting,” in *Computer Vision—ECCV 2020: 16th European Conference, Glasgow, UK, August 23–28, 2020, Proceedings, Part II 16*. Springer, 2020, pp. 541–556.
- [32] E. Brockfeld, R. D. Kühne, A. Skabardonis, and P. Wagner, “Toward benchmarking of microscopic traffic flow models,” *Transportation research record*, vol. 1852, no. 1, pp. 124–129, 2003.
- [33] N. Nayakanti, R. Al-Rfou, A. Zhou, K. Goel, K. S. Refaat, and B. Sapp, “Wayformer: Motion forecasting via simple & efficient attention networks,” in *2023 IEEE International Conference on Robotics and Automation (ICRA)*. IEEE, 2023, pp. 2980–2987.
- [34] Y. Gao, Z. Chen, J. Wang, X. Zhang, and Y. Zhang, “Vectornet: Encoding hd maps and agent dynamics from vectorized representation,” *arXiv preprint arXiv:2006.05262*, 2020.
- [35] J. Ho, A. Jain, and P. Abbeel, “Denoising diffusion probabilistic models,” *Advances in neural information processing systems*, vol. 33, pp. 6840–6851, 2020.
- [36] W. Peebles and S. Xie, “Scalable diffusion models with transformers,” in *Proceedings of the IEEE/CVF International Conference on Computer Vision*, 2023, pp. 4195–4205.
- [37] A. Vaswani, N. Shazeer, N. Parmar, J. Uszkoreit, L. Jones, A. Gomez, L. Kaiser, and I. Polosukhin, “Attention is all you need,” *Advances in neural information processing systems*, pp. 5998–6008, 2017.
- [38] K. Cho, B. Van Merriënboer, C. Gulcehre, D. Bahdanau, F. Bougares, H. Schwenk, and Y. Bengio, “Learning phrase representations using rnn encoder-decoder for statistical machine translation,” *Computer Science*, 2014.
- [39] P.-E. Casas, J. Hsu, J. Kuderer, and P. Abbeel, “Multipath: Modelling multiple future driving paths with anchor trajectories,” *arXiv preprint arXiv:1904.01124*, 2019.
- [40] J. H. Friedman, “Greedy function approximation: A gradient boosting machine,” *Annals of Statistics*, vol. 29, no. 5, pp. 1189–1232, 2001.
- [41] Waymo, “Waymo open dataset,” <https://waymo.com/open/data/motion/>, 2021.
- [42] N. Montali, J. Lambert, P. Mougin, A. Kuefler, N. Rhinehart, M. Li, C. Gulino, T. Emrich, Z. Yang, S. Whiteson *et al.*, “The waymo open sim agents challenge,” *arXiv preprint arXiv:2305.12032*, 2023.
- [43] J. Gil, L. Martín, C. Montes, and A. Ortega, “A fast procedure for computing the distance between complex objects in three-dimensional space,” *Computer graphics forum*, vol. 10, no. 4, pp. 331–340, 1991.
- [44] D. Kingma and J. Ba, “Adam: A method for stochastic optimization,” *Computer Science*, 2014.
- [45] I. Loshchilov and F. Hutter, “Sgdr: Stochastic gradient descent with warm restarts,” *arXiv e-prints*, vol. abs/1608.03983, 2016.
- [46] S. Shi, L. Jiang, D. Dai, and B. Schiele, “Mtr++: Multi-agent motion prediction with symmetric scene modeling and guided intention querying,” *arXiv preprint arXiv:2306.17770*, 2023.
- [47] L. Jiang, D. Chen, Z. Li, and Y. Wang, “Risk representation, perception, and propensity in an integrated human lane-change decision model,” *IEEE Transactions on Intelligent Transportation Systems*, vol. 23, no. 12, pp. 23 474–23 487, 2022.